PAKISTAN JOURNAL OF EMERGING SCIENCE AND TECHNOLOGIES (PJEST)

December, 2022, 3(2) ISSN 2788-8630 (On-Line)

TUNING OF HYDROXYAPATITE WITH NANOPARTICLES OF MULTIPLE METAL OXIDES

Nimra Ehsan[1]*, Faiza Hassan[1], Maira Ehsan[2]

[1] Department of Chemistry, University of Lahore, Lahore, Pakistan

[2] Centre of excellence of solid state physics, University of the Punjab, Lahore, Pakistan

*Corresponding Author: Nimra Ehsan, email: nimra.ehsan@chem.uol.edu.pk

ARTICLE INFORMATION

Crossref DOI:

https://doi.org/10.58619/pjest.v3i2.79

Received: 5th January-2023

Revised and Accepted:

6th-January-2023

Published On-Line

21st -January-2023

***Corresponding Author:**

Nimra Ehsan, email: nimra.ehsan@chem.uol.edu.pk

Original Research Article

ABSTRACT

Fabrication and commercial application of nano-hydroxyapatite synthetic bioceramic compound is being implemented immensely worldwide in medicine, dentistry, and ceramic industries. In this experimental study, nano-hydroxyapatite has been prepared through the sol-gel method and doped with nano-silica, nano-alumina, and sodium zeolite. The main objective of this study is to improve the properties of nano-hydroxyapatite doped with nanoparticles of different metal oxides for load-bearing orthopaedic applications. The metal oxides have been doped in pure nano-hydroxyapatite by two different methods: physical attachment and chemical methods. After blending these metal oxides in nano-hydroxyapatite powder, comprehensive characterizations of compositional, structural, morphological, thermal, and mechanical properties have been determined through X-ray diffraction, Scanning Electron Microscope, Raman Spectroscopy, Thermogravimetric Analysis, respectively. The experimental outcomes revealed that all properties of the nano-hydroxyapatite material have been improved significantly with doping of metal oxides while nano-alumina was the most effective metal oxide.

Keywords: Nano-Hydroxyapatite (nHA), Metal oxides, X-ray Diffraction (XRD), Raman Spectroscopy, Thermogravimetric Analysis (TGA), Scanning Electron Microscope (SEM)

Introduction:

Various bio-ceramic materials are investigated due to their direct connotation with human health [1-3]. Calcium phosphate and hydroxyapatite is the prominent examples of bioactive materials which are used for bone replacement [4, 5]. Hydroxyapatite is an artificial bone material that has a close resemblance to the bones due to the presence of calcium and phosphorous [2, 5-14]. Calcium phosphate ceramics, particularly nano-hydroxyapatite (nHA) ($Ca_{10}(PO_4)_6(OH)_2$) is the most suitable inorganics material which is used as a bone substituent due to its biological and chemical compositions similar to natural bone. nHA is an integral part of human teeth and bones, which is accounted for 96% weight of teeth and 72% weight of bones [5-14]. It is created a strong chemical bond interaction with bone tissues due to its biocompatibility, highly bioactive, osteo-conductivity, bio-inertness, sterilization, and bio functionality [14, 15]. nHA is also used as a drug release agent for cell loading,

chromatography analysis, and rigid tissue scaffolding [8, 11, 14, 16]. It is extensively doped with different metal oxides to obtain its osteo-conductivity and bioactive phase [16]. However, stoichiometric hydroxyapatite has generally low capacity to connect with existing bone, staying as a perpetual installation helpless too long-haul disappointment. The elements nano-silica, nano-alumina, and sodium zeolite play an essential role in the chemistry of teeth and bones. These substituents can influence the surface structure and charge of hydroxyapatite, prompting an effect on the material in a natural condition [17, 18].

Some previous studies [17, 19, 20] presented that silicate ion or silicon replaces phosphate or phosphorous ion with the subsequent loss of charge equilibrium. In this regard, the bioactivity of hydroxyapatite can be enhanced with the doping of silicon in hydroxyapatite. However, the doping of nano-silica to hydroxyapatite does not result in the thermal instability of silicon doped hydroxyapatite. Therefore, the purpose of this research work is to bring out the state and solubility limit of silicon, nano-alumina, and zeolite doped-hydroxyapatite synthesized by the sol-gel method by using the same contents of nano-silica, nano-alumina, and sodium zeolite separately and in combined form. Chemical characterization of these metal oxides doped hydroxyapatite has been carried out.

Nano-alumina Al_2O_3 has occurred in different forms of natural minerals such as corundum (Al_2O_3). The chemical, electrical and mechanical properties of nano-alumina used in ceramic industries are investigated. Nano-alumina is used as an insulating material due to its excellent thermal and dielectric properties. Nano-alumina is also used as a biomaterial substitute to replace joints, used to implant cochlear [18, 21, 22].

Zeolite is extensively used in industries due to its adaptability, flexibility, adsorbents ability, ion exchange, and molecular filters. It is used for the in-vivo and in-vitro study of cancer disease and decreases the cancer tumor [23-25].

The main objective of this investigation is to enhance the nHA properties for commercial application using a quick methodology route commonly named a sol-gel method [6, 26-28]. By the addition of different metal oxides, the hardness, stability, and mechanical strength of nHA have been improved notably which makes it suitable for load-bearing orthopaedic applications [28]. This study also investigated how the stirring time and sintering temperature in the sol-gel method affect the particle size of nHA. The novelty of this research is that nHA powder produced via the sol-gel method has been doped with three metal oxides: nano-silica, nano-alumina, and sodium zeolite which has not been experimented with earlier. To the author's best knowledge, this is the first study on nHA doped with nano-silica, nano-alumina, and sodium zeolite for biomedical implementations.

Materials and Methods

At temperatures between 900C and 1200C, hydroxyapatite nanopowder (nHA) was synthesized using the sol-gel method. In this synthetic procedure, the initial Ca and P precursors were Na_2HPO_4 and $Ca(NO_3)_2$. As doping metal oxides, sodium zeolite, nano-silica, and nano-alumina were utilized. Na_2HPO_4 was dissolved in 100mL water and put in the beaker on the hot plate for continuous stirring at the temperature of 90^0C to 120^0C. In another beaker, a 1.67 M $Ca(NO_3)_2$ solution containing 50mL water was prepared. During the process of constantly magnetic stirring, 1.67 M $Ca(NO_3)_2$ solution was added drop-by-drop to the 1 M Na_2HPO_4 solution to achieve the Ca/P=1.67. The 100 mL of water and the citric acid solution was dissolved in the primary solution. After 60 minutes, it was observed that the solution's pH was acidic. To change the pH of the primary solution, a solution of NaOH pellets in 50mL water was made and added gradually. It was noted that the pH of the final solution is 8. After constant stirring for around 40 minutes, the final solution converted to gel.

The gel form was taken off the hot plates and allowed to cool at room temperature. This gel form was converted into a solid form after the evaporation of its solvent. This dense form was ground in a ceramic mortar, and the compact solid mass of hydroxyapatite was collected.

One sample of the ground form of nHA was air dried at ambient temperature for 72 hours to create the powdered form, while the other sample was heated in a furnace to 800°C with 10°C increments per minute. With sintered nHA, three distinct metal oxides nano-silica, nano-alumina, and sodium zeolite were attached in two separate ways: chemically and physically. Each of these procedures produced four samples of doped nHA. In the physical attachment process, three samples of doped nHA were prepared by mixing the prepared nHA with each metal oxide separately with a ceramic mortar. The fourth sample was also prepared by mixing all three metal oxides in nHA in a ceramic mortar. In the chemically attached process, metal oxides were solubilized into deionized water. Three doped nHA were prepared by doping solubilized metal oxides separately in gel form of nHA during the synthesis process. The fourth sample was also prepared by doping all three metal oxides into the gel form of nHA. All these samples were sintered at a temperature of 10^0C increment/min to 800 ^{0}C for two hours. Finally, this thermally treated material was crushed with the help of a ceramic mortar.

Characterization Techniques

X-ray diffractometer was utilized to evaluate the crystalline size by using Cuka radiation of wavelength 1.5405 and identify the crystalline phase transformation of the material. All the samples were scanned at the range of 5^0-80^0 at 2θ with a scanning speed of 1^0/s. Scherer's formula [16] presented in Eq.1 was used to determine the crystalline size.

$$D = 0.89\lambda / d\cos\theta \qquad \text{(Eq.1)}$$

Where, λ = 1.54060 for Cuka, d=FWHM, and D= size of the particle.

The calculated grain size of the sintered sample and air-dried samples of nHA are 48 nm and 52 nm, respectively.

Scanning electron (SEM) was used to study morphology and calculate the grain size of the particles. Compositional analysis, thermal stability, and oxidative stability of the material were studied using thermogravimetric analysis (TGA) up to 1200^0C temperature. The Raman spectrometer technique is used to identify and analyze the molecular structure of the material.

Results and Discussion

In this analysis, initially, molecular structures of two undoped samples nHA, air-dried and sintered, were studied through the Raman Spectroscopy technique under the free oxygen environment. These samples were exposed to ultrahigh radiations for 30 sec.

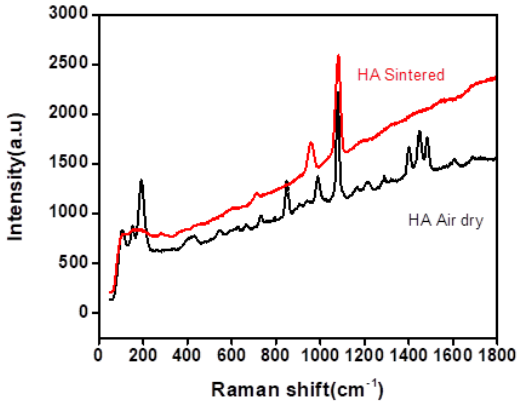

Figure 1: Raman Spectroscopy results of air-dried nHA and sintered nHA

From **Figure 1**, the Raman peaks of all functional groups of hydroxyapatite such as PO_4^{-3}(P-O Stretching), PO_4^{-3}(P-O Bending), phosphate ion vibration, hydroxyl (OH), and carbonate ion are confirmed for both samples. It is also found that the single peak of the hydroxyl group is observed at 1075 cm-1 in the case of the sintered sample compared to the dried sample, which contains multiple hydroxyl peaks due to the access amount of water and impurities.

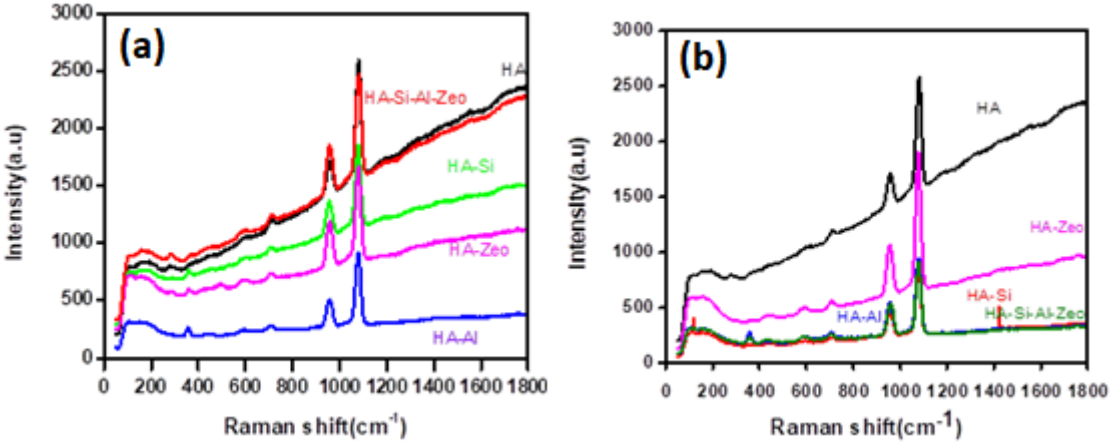

Figures (**2a** and **2b**) showed the Raman peaks of sintered nHA samples and metal-doped nHA samples.

The Raman peak of nHA is observed in the range of 950-960 cm^{-1} and 1075 cm^{-1}, nHA-SiO_2 in the range of 350-400 cm^{-1}, nHA- Al_2O_3 at 360 cm^{-1} , nHA-Na-Zeolite at 360 cm^{-1} and in the range of 650-790 cm^{-1} and nHA- SiO_2-Al_2O_3-NaZeolite sample in the range of 350-400 cm^{-1}, 650-790 cm^{-1}, 950-960 cm^{-1}, 1075 cm^{-1}. In the case of the chemical process the Raman peas are observed nHA n the range of 950-960 cm^{-1} and 1075 cm^{-1}, nHA-SiO_2 at 960 cm^{-1}, nHA-Al_2O_3 at 360 cm^{-1} , nHA-Na-Zeolite in the range of 590-706 cm^{-1} and nHA- SiO_2-Al_2O_3-Na-Zeolite sample in the range of 350-400 cm^{-1}, 650-790 cm^{-1}, 950-960 cm^{-1}, 1075 cm^{-1}. The above data confirm the presence of apatite peaks at 1075 cm^{-1} at different intensities in each sample. The peak observed at 960 cm^{-1} in the sample of nHA-SiO_2 confirms the substitution of SiO_2 with phosphate ion.

In **Figure 3**, the characteristic peak of sintered sample is observed within the reference range 31.5-32.8^0 of the apatite phase, whereas the peak of air-dried sample is observed at 30^0.

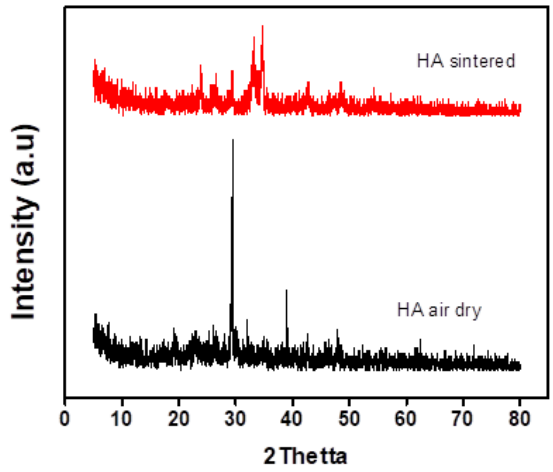

Figure 3: XRD Pattern of Hydroxyapatite air-dried and sintered

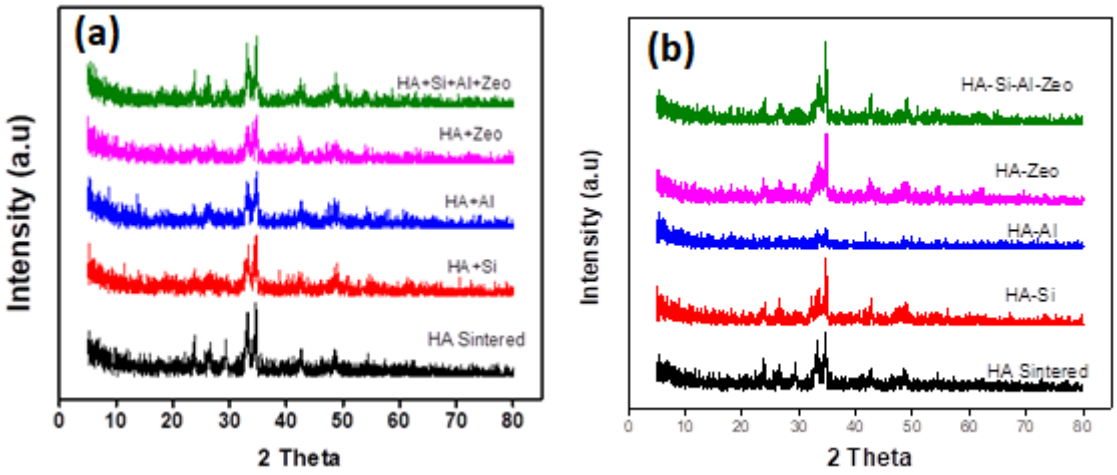

Figure 4(a) and 4(b): XRD pattern of (a) physically (b) chemically, prepared nHA and nHA doped with silica, alumina, and zeolite metals oxides

After studying the XRD pattern from **Figures 3** and **4 (a),(b)**, it was observed that the characteristic peak of the apatite phase at 31.5^0 -32.8^0 is present in all samples of nHA doped with metal oxides. The Al_2O_3 diffraction peaks are observed between 25^0 -35^0. the diffraction peak of zeolite is observed at 34.5^0 following the structure and crystallinity of nHA. The peaks observed at different diffraction patterns at about 170, 210, 250, and 530 are due to change in the secondary phase of hydroxyapatite due to doping with various metal oxides crystallinity and grain size. In the second experiment, the samples are prepared by the sol-gel method, and metal oxides are doped during the synthesis of nHA. The purpose of this doping is to change the crystal structure, grain size, and porosity of the desired nHA. From the data given above, it is investigated that in all samples including pure nHA and doping of metal oxides oxide. The characteristic diffraction peaks of nHA are observed at $32^{0,}$ which shows the presence of the apatite phase. The diffraction peaks of others metal oxides are also observed as nanosilica at 41.3^0, nanoalumina at $25^{0,}$ and Na-zeolite at 35^0-40^0. The formation of other peaks at different diffraction patterns shows the formation of the secondary phase of nHA and the substitution of the phosphate group of nHA with nano-silica or nano-alumina.

SEM is a morphological study of materials used for imaging purposes. We can find out the crystallinity, porosity, and size of crystal structures by using SEM techniques. In this research, the SEM results obtained for different samples are in good agreement with previous

literature. These fine images of the material samples are obtained under the magnification of 5000, 10000, 24000, and 40000. These images show the excellent crystal structure of different scales of particle sizes.

In this research, ten samples of pure nHA and nHA doped with metal oxides (Nano-Alumina, Nano-Silica, Na-Zeolite) by using SEM have been investigated. **Figures 6-8** present the SEM images of these samples. **Figures 6-8** presented that the prepared samples contain a coagulated surface with a smooth surface, homogeneous layered crystal, and porous structure, irregular grain size, and needle-like structure with the agglomeration of nano-hydroxyapatite powder and fibre-like morphology appears in doped samples. These results also showed that the crystallinity of nano-powder enhances, and porosity decreases due to the doping of metal oxides in nHA.

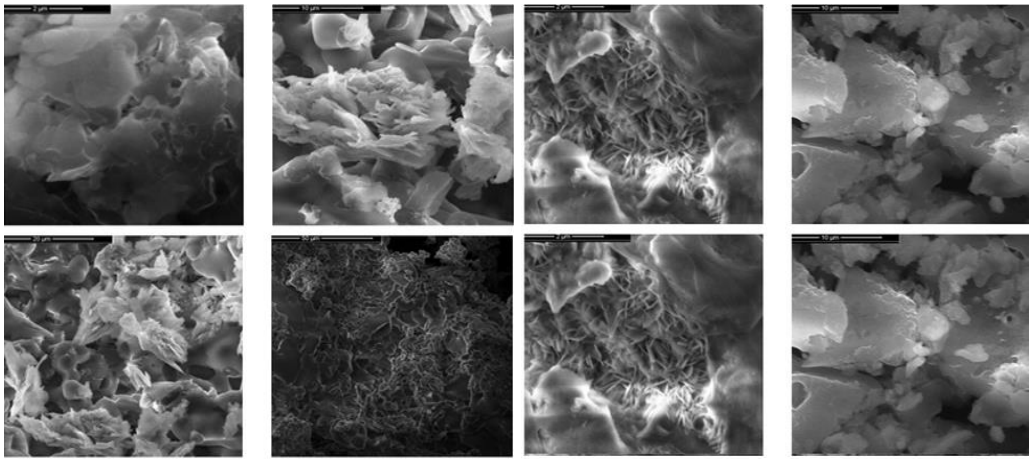

(a) **(b)**

Figure 6: SEM results of **(a)** air-dried and **(b)** sintered nHA Samples

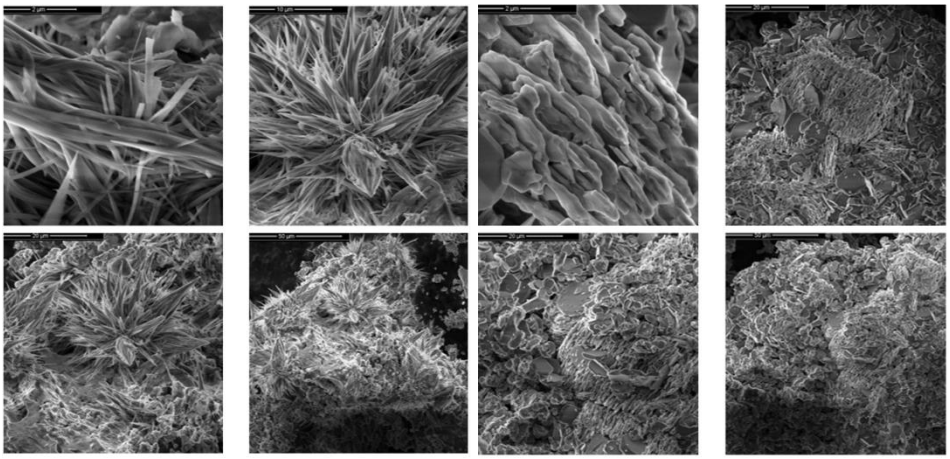

(a) **(b)**

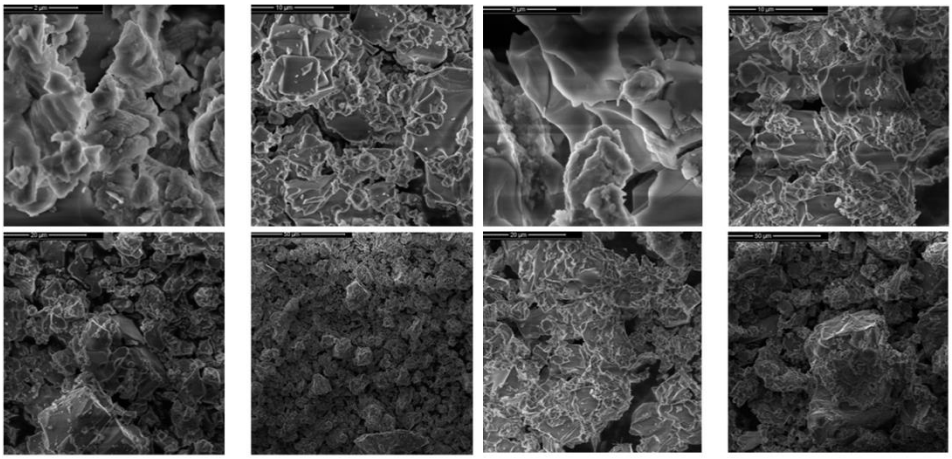

(c) **(d)**

Figure 7: SEM results of physically prepared nHA doped with metal oxide **(a)** Nano-silica **(b)** Nano-alumina **(c)** Na-zeolite **(d)** Mixed Nano-silica+nano-alumnia+Na-zeolite

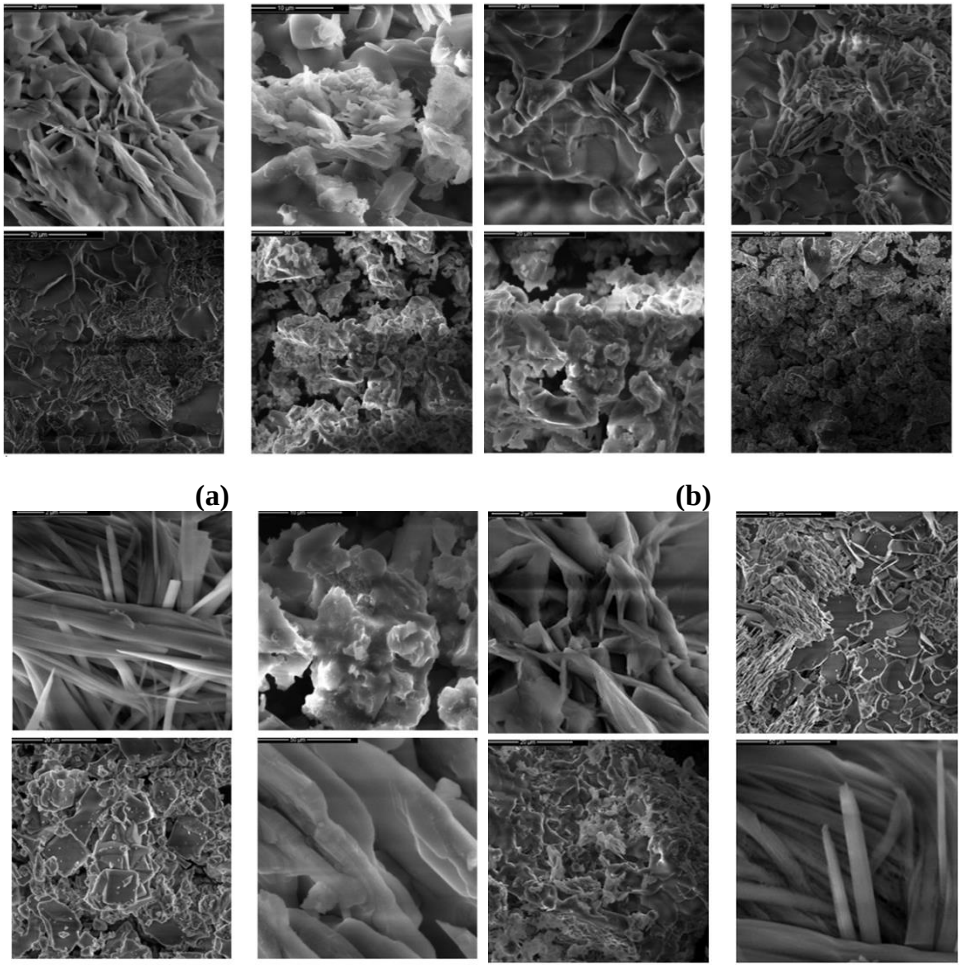

(a) **(b)**

(c) **(d)**

Figure 8: SEM results of chemically prepared nHA doped with metal oxide **(a)** Nano-silica **(b)** Nano-alumina **(c)** Na-zeolite **(d)** Mixed Nano-silica+nano-alumnia+Na-zeolite

Thermogravimetric analysis is a thermal treatment of materials in which the physical and chemical properties of materials are changed due to heat. In TGA results, loss in weight percentage versus increase in temperature is measured. SnHAes of TGA curves explains the destabilization of materials.

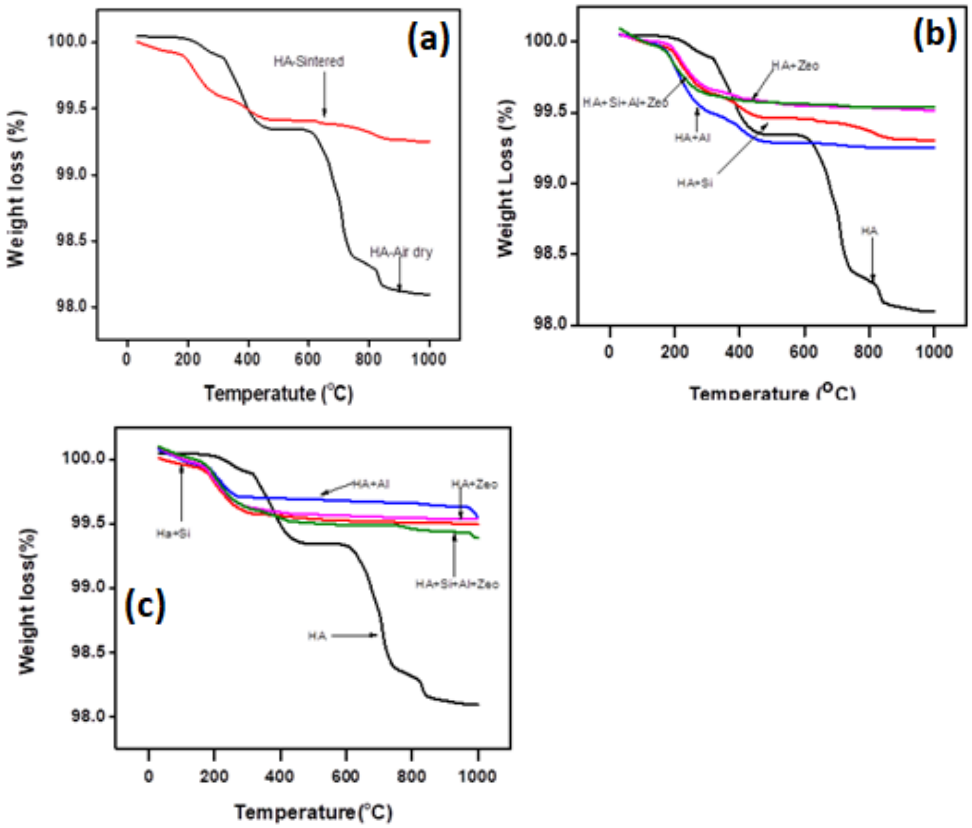

Figure 9: TGA results of **(a)** air-dried Hydroxyapatite and Sintered Hydroxyapatite **(b)** physically **(c)** chemically, prepared nHA doped with metal oxides (Nano-Alumina, Nano-Silica, Na-Zeolite)

Table1: TGA results of Air Dried HA and Sintered HA

Sr. No.	**Degradation Temperature (^{0}C)**	**Weight Loss (%)**
Air Dried Hydroxyapatite	0-170	Stable
	320	0.8
	320-485	1.5
	480-600	Stable
	780-800	2
	Above 800	Stable
Maximum weight loss occurs at 2% at 800 ^{0}C		
Sintered Hydroxyapatite	0-170	0.1
	315	0.15
	400-650	Stable
	800-900	1
	Above 900	Stable
Maximum weight loss occurs at 1% at 900 ^{0}C		

Table2: TGA results of physically prepared HA with metal oxides SI, Al, and Zeolite

Sr. No.	**Degradation Temperature (^{0}C)**	**Weight Loss (%)**
HAP + Nano-Silica	0-190	0.07
	320	0.37
	470	0.55
	850	0.67
	Above 900	Stable
Maximum weight loss occurs at 0.67% at 850 ^{0}C		
HAP + Nano-Alumina	0-180	0.01
	290	0.05

	480	0.72
	490-900	Stable
Maximum weight loss occurs at 0.72% at 480 ^{0}C		
HAP + Zeolite	0-175	0.01
	280	0.33
	320-900	Stable
Maximum weight loss occurs at 0.33% at 280 ^{0}C		
HAP + Al + Si + Zeolite	0-170	0.07
	280	0.36
	Above 400	Stable
Maximum weight loss occurs at 0.36% at 280 ^{0}C		

Table3: TGA results of chemically prepared HA with metal oxides SI, Al, and Zeolite

Sr No.	**Degradation Temperature (^{0}C)**	**Weight Loss (%)**
HAP + Nano-Silica	0-135	0.07
	320	0.41
	Above 380	Stable
Maximum weight loss occurs at 0.41% at 320 ^{0}C		
HAP+ Nano-Alumina	0-160	0.04
	320	0.41
	Above 350	Stable
Maximum weight loss occurs at 0.41% at 320 ^{0}C		
HAP + Zeolite	0-170	0.05
	270	0.31
	300-900	0.35
	Above 900	Stable
Maximum weight loss occurs at 0.35% at 300-900 ^{0}C		
HAP + Al + Si + Zeolite	0-190	0.01
	270	0.35
	420	0.48
	780	0.51
	790-960	Stable
	960-1000	0.62
Maximum weight loss occurs at 0.62% at 960-1000 ^{0}C		

Table 4: Hardness of all samples

Sr#	**Samples**	**Process**	**Hardness GPa**
1	Air Dried		12.4
2	Sintered		14.8
3	nHA+nano-Silica	Physically attachment	13.6
4	nHA+nano-Alumina	Physically attachment	16.7
5	nHA+nano-Na-Zeolite	Physically attachment	10.2
6	nHA+nano-Silica+Alumina+Na-Zeolite	Physically attachment	14.2
7	nHA+nano-Silica	Chemically attachment	15.6
8	nHA+nano-Alumia	Chemically attachment	16.8

9	nHA+nano-Na-Zeolite	Chemically attachment	13.2
10	nHA+nano-Silica+Alumina+Na-Zeolite	Chemically attachment	15.4

The hardness of sintered hydroxyapatite was found high as compared to air dried sample. It is also observed that the nano-hydroxyapatite samples prepared by chemical attachment were shown high hardness as compared to physically attached samples. The alumina doped sample has the highest values of hardness. Our nHA+alumina and nHA+silica have high values of hardness as compared to alumina 1.03 GPa [29] and silica 6.73 GPa [30].

Conclusion

In this research work, porous hydroxyapatite was prepared by using sol-gel method. Synthesized nHA was dried in two different ways, an air-dried sample and a thermally treated sample kept in a furnace at 800^0C for two hours. These fabricated nHA samples were characterized by using various characterization techniques Raman, XRD, SEM, and TGA. The pure phase of nHA was observed in all samples after the characterization process. Raman spectra showed the presence of water in the dried air sample. By analyzing the TGA curve of air-dried sample, a high percentage of weight loss was observed due to the loss of water and other impurities present in the air-dried sample. High stability of the nHA was observed sintered sample, and no water molecules were observed after the characterization. The grain size of air-dried and sintered samples was determined at 50 nm and 48 nm, respectively, by using the Scherer formula.

Eight samples of sintered porous hydroxyapatite, nHA doped with nano-silica, nHA doped with nano-alumina, nHA doped with Zeolite, and nHA doped with all three metal oxides, were prepared by using two different methods, physical attachment and chemical treatment separately. In the physical attachment process, four samples nHA doped with these metal oxides were prepared after mixing them in a ceramic mortar. On the other hand, four samples were prepared after mixing these metal oxides in nHA gel during the synthesis process. These all samples were characterized by using various characterization techniques Raman, XRD, SEM, and TGA. These characterizations showed that the properties of nHA enhanced with the doping of these metal oxides. Raman peaks and XRD patterns revealed the presence of nHA and these metal oxides. Extraordinary SEM results were obtained, which show the fine needle and flower-like crystal structures of the material. TGA curves revealed the high stability of nHA doped with these metal oxides samples.

Author's Contribution: N. Ehsan synthesized, and analyzed results. Interpretation of data and writing the basic draft, F. Hassan supervised and critical revision, M. Ehsan assisted to manage the graphical data.

Funding: The publication of this article was funded by no one.

Conflicts of Interest: The authors declare no conflict of interest.

REFERENCES

[1] M. A. F. Afzal, S. Kalmodia, P. Kesarwani, B. Basu, and K. Balani, "Bactericidal effect of silver-reinforced carbon nanotube and hydroxyapatite composites," *Journal of biomaterials applications,* vol. 27, pp. 967-978, 2013.

[2] M. Ji, H. Li, H. Guo, A. Xie, S. Wang, F. Huang, *et al.*, "A novel porous aspirin-loaded (GO/CTS-HA) n nanocomposite films: Synthesis and multifunction for bone tissue engineering," *Carbohydrate polymers,* vol. 153, pp. 124-132, 2016.

[3] M. Kikuchi and D. Kanama, "Current status of biomaterial research focused on regenerative medicine," NISTEP Science & Technology Foresight Center 1349-3663, 2007.

[4] W. Suchanek and M. Yoshimura, "Processing and properties of hydroxyapatite-based biomaterials for use as hard tissue replacement implants," *Journal of materials research,* vol. 13, pp. 94-117, 1998.

[5] I. Sopyan, M. Mel, S. Ramesh, and K. Khalid, "Porous hydroxyapatite for artificial bone applications," *Science and Technology of Advanced Materials,* vol. 8, p. 116, 2007.

[6] D. Gopi, S. Nithiya, L. Kavitha, and J. Ferreira, "Amino acid-assisted synthesis of strontium hydroxyapatite bone cement by a soft solution freezing method," *Bulletin of Materials Science,* vol. 35, pp. 1195-1199, 2012.

[7] M. J. Hossan, M. Gafur, M. Karim, and A. Rana, "Mechanical properties of Gelatin Hydroxyapatite composite for bone tissue engineering," *Bangladesh Journal of Scientific and Industrial Research,* vol. 50, pp. 15-20, 2015.

[8] D. Liu, Z. Liu, J. Zou, L. Li, X. Sui, B. Wang, *et al.*, "Synthesis and characterization of a hydroxyapatite-sodium alginate-chitosan scaffold for bone regeneration," *Frontiers in Materials,* vol. 8, p. 648980, 2021.

[9] Y. Liu and M. Wang, "Fabrication and characteristics of hydroxyapatite reinforced polypropylene as a bone analog biomaterial," *Journal of applied polymer science,* vol. 106, pp. 2780-2790, 2007.

[10] M. Mudhafar, I. Zainol, H. Alsailawi, and C. Aiza Jaafar, "Synthesis and characterization of fish scales of hydroxyapatite/collagen–silver nanoparticles composites for the applications of bone filler," *Journal of the Korean Ceramic Society,* vol. 59, pp. 229-239, 2022.

[11] O. A. Osuchukwu, A. Salihi, I. Abdullahi, B. Abdulkareem, and C. S. Nwannenna, "Synthesis techniques, characterization and mechanical properties of naturally derived hydroxyapatite scaffolds for bone implants: a review," *SN Applied Sciences,* vol. 3, pp. 1-23, 2021.

[12] A. Pangon, S. Saesoo, N. Saengkrit, U. Ruktanonchai, and V. Intasanta, "Hydroxyapatite-hybridized chitosan/chitin whisker bio-nanocomposite fibers for bone tissue engineering applications," *Carbohydrate polymers,* vol. 144, pp. 419-427, 2016.

[13] J. H. Patil, K. Vishnumurthy, R. Kusanur, and R. Melavanki, "Synthesis and characterization of chitosan-hydroxyapatite composite for bone graft applications," *Journal of the Indian Chemical Society,* vol. 99, p. 100308, 2022.

[14] S. Saravanan, R. Leena, and N. Selvamurugan, "Chitosan-based biocomposite scaffolds for bone tissue engineering," *International journal of biological macromolecules,* vol. 93, pp. 1354-1365, 2016.

[15] S. Gorgieva and V. Kokol, "Collagen-vs. gelatine-based biomaterials and their biocompatibility: review and perspectives," *Biomaterials applications for nanomedicine,* vol. 2, pp. 17-52, 2011.

[16] G. Devanand Venkatasubbu, S. Ramasamy, G. Avadhani, L. Palanikumar, and J. Kumar, "Size-mediated cytotoxicity of nanocrystalline titanium dioxide, pure and zinc-doped hydroxyapatite nanoparticles in human hepatoma cells," *Journal of Nanoparticle Research,* vol. 14, pp. 1-18, 2012.

[17] X. L. Tang, X. F. Xiao, and R. F. Liu, "Structural characterization of silicon-substituted hydroxyapatite synthesized by a hydrothermal method," *Materials Letters,* vol. 59, pp. 3841-3846, 2005.

[18] M. A. Islam, D. W. Morton, B. B. Johnson, B. K. Pramanik, B. Mainali, and M. J. Angove, "Metal ion and contaminant sorption onto aluminum oxide-based materials: A review and future research," *Journal of environmental chemical engineering,* vol. 6, pp. 6853-6869, 2018.

[19] K. Nakata, T. Kubo, C. Numako, T. Onoki, and A. Nakahira, "Synthesis and characterization of silicon-doped hydroxyapatite," *Materials transactions,* pp. 0902160670-0902160670, 2009.

[20] A. Yacoubi, A. Massit, M. Fathi, B. Chafik, E. Idrissi, and K. Yammi, "Characterization of silicon-substituted hydroxyapatite powders synthesized by a wet precipitation method," *Journal of Applied Chemistry,* vol. 7, pp. 24-29, 2014.

[21] A. Fahami, B. Nasiri-Tabrizi, G. W. Beall, and W. J. Basirun, "Structural insights of mechanically induced aluminum-doped hydroxyapatite nanoparticles by Rietveld refinement," *Chinese journal of chemical engineering,* vol. 25, pp. 238-247, 2017.

[22] S. Vignesh Raj, M. Rajkumar, N. Meenakshi Sundaram, and A. Kandaswamy, "Synthesis and characterization of hydroxyapatite/alumina ceramic nanocomposites for biomedical applications," *Bulletin of Materials Science,* vol. 41, pp. 1-8, 2018.

[23] N. Iqbal, M. A. Kadir, S. Iqbal, S. I. Abd Razak, M. S. Rafique, H. Bakhsheshi-Rad, *et al.,* "Nano-hydroxyapatite reinforced zeolite ZSM composites: A comprehensive study on the structural and in vitro biological properties," *Ceramics International,* vol. 42, pp. 7175-7182, 2016.

[24] Y. Kuwahara, T. Ohmichi, T. Kamegawa, K. Mori, and H. Yamashita, "Synthesis of hydroxyapatite–zeolite composite material from disposed steel slag and investigation of its structural and physicochemical characteristics," *Chemistry Letters,* vol. 38, pp. 626-627, 2009.

[25] Y. Zhan, J. Lin, and J. Li, "Preparation and characterization of surfactant-modified hydroxyapatite/zeolite composite and its adsorption behavior toward humic acid and copper (II)," *Environmental science and pollution research,* vol. 20, pp. 2512-2526, 2013.

[26] G. Bezzi, G. Celotti, E. Landi, T. La Torretta, I. Sopyan, and A. Tampieri, "A novel sol–gel technique for hydroxyapatite preparation," *Materials Chemistry and Physics,* vol. 78, pp. 816-824, 2003.

[27] O. Osuchukwu, A. Salihi, I. Abdullahi, and D. Obada, "Synthesis and characterization of sol–gel derived hydroxyapatite from a novel mix of two natural biowastes and their potentials for biomedical applications," *Materials Today: Proceedings,* 2022.

[28] H. Belhouchet, F. Chouia, M. Hamidouche, and A. Leriche, "Preparation and characterization of anorthite and hydroxyapatite from Algerian kaolin and natural phosphate," *Journal of Thermal Analysis and Calorimetry,* vol. 126, pp. 1045-1057, 2016.

[29] M. Aminzare, A. Eskandari, M. Baroonian, A. Berenov, Z. R. Hesabi, M. Taheri, *et al.,* "Hydroxyapatite nanocomposites: Synthesis, sintering and mechanical properties," *Ceramics International,* vol. 39, pp. 2197-2206, 2013.

[30] R. Tolouei, C. Y. Tan, R. Singh, I. Sopyan, and W. D. Teng, "Effect of nano silica on the sinterability of hydroxyapatite dense bodies," in *Advanced Materials Research*, 2011, pp. 1832-1838.